# Formation of a Boundary-Free Dust Cluster in a Low-Pressure Gas-Discharge Plasma

A. D. Usachev,[1,*,†] A. V. Zobnin,[1] O. F. Petrov,[1] V. E. Fortov,[1] B. M. Annaratone,[2] M. H. Thoma,[3] H. Höfner,[3] M. Kretschmer,[3] M. Fink,[3] and G. E. Morfill[3]

[1]*Joint Institute for High Temperatures of Russian Academy of Sciences, Moscow, 125412, Russia*
[2]*CNRS/Université de Provence, Centre de St. Jêrome case 321, 13397, Marseille, France*
[3]*Max-Planck-Institut für extraterrestrische Physik, P.O. Box 1321, D- 85741 Garching, Germany*

(Received 20 March 2006; revised manuscript received 13 March 2008; published 26 January 2009)

An attraction between negatively charged micron-sized plastic particles was observed in the bulk of a low-pressure gas-discharge plasma under microgravity conditions. This attraction had led to the formation of a boundary-free dust cluster, containing one big central particle with a radius of about 6 $\mu$m and about 30 1 $\mu$m-sized particles situated on a sphere with a radius of 190 $\mu$m and with the big particle in the center. The stability of this boundary-free dust cluster was possible due to its confinement by the plasma flux on the central dust particle.

DOI: 10.1103/PhysRevLett.102.045001 PACS numbers: 52.27.Lw, 52.27.Gr

Micron-sized dust particles injected into a low temperature discharge plasma quickly acquire a large negative electric charge and form dusty plasma structures [1,2]. The strong electrostatic repulsion between the charged dust particles tends to a dispersion of such structures. For the confinement of the structures usually external electrostatic traps are used. Such traps are naturally formed in the plasma sheath [1], in a diffuse plasma edge, as well as in dc strata [2], i.e., in rather disturbed regions of the discharge plasmas. The formation of so-called boundary-free dust structures, i.e., dust clouds in a uniform bulk plasma without external electrostatic traps, is of great scientific interest [3]. Such structures would exist if attractive forces between negatively charged dust particles are present in the bulk plasma. The existence of such attractive forces was originally predicted by Tsytovich [4] and Ignatov [5], who considered an attraction of two dust particles due to mutual shadowing of plasma flows on these particles. The conditions where the collective attraction dominates can be estimated as $r_p^2/r_{\mathrm{D}i}^2 \gg T_i/T_e$, where $r_p$ and $r_{\mathrm{D}i}$ are the dust particle and Debye radii, respectively [3]. For typical dusty plasma experiments in low-pressure gas-discharge plasmas, $T_i/T_e \sim 0.01$ and $n_{i0} \sim 10^{15}$ m$^{-3}$, the radius of the particles should be larger than 4 $\mu$m. Hence, for the formation of boundary-free structures it is necessary to use either relatively big ($r_p > 5$–$10$ $\mu$m) particles or dense plasmas ($n_i$, $n_e \gg 10^{15}$ m$^{-3}$). Unfortunately, large dust particles do not levitate in lab experiments due to their relatively large weight. On the other hand, a high plasma density leads to strong plasma flows to the chamber walls. These flows quickly push out the dust cloud from the bulk plasma to the chamber walls and cause void formation [6]. Because of these experimental problems the boundary-free dust structures have not yet been directly observed. Meanwhile, an attraction between negatively charged particles and negatively charged macroscopic objects in a plasma was experimentally observed in [7,8], which indirectly confirms the possibility of the existence of boundary-free structures. Note that "wake clusters" [9] cannot be treated as boundary-free structures as they exist only in anisotropic plasmas.

In the present work, the above mentioned experimental problems have been eliminated by using a combined dc-rf gas discharge in the "Plasmakristall-4" (PK-4) setup [10] under microgravity conditions and applying rf pulses. The experiments were performed in the PK-4 chamber during the 41st European Space Agency parabolic flight campaign in October 2005 onboard the A-300 ZERO-G plane. The experimental arrangement (Fig. 1) consists of the Π-shape glass discharge tube of 30 mm inner diameter with a total length of 85 cm filled by neon at a pressure of 60 Pa. The tube is equipped with two dc cylindrical electrodes installed at the ends of the tube. The dc discharge was operated at $I_{\mathrm{dc}} = 1.0$ mA and $U_{\mathrm{dc}} = 884$ V, and its uniform positive column filled almost the entire chamber volume. In addition to the dc electrodes, the PK-4 discharge chamber was equipped with an rf coil installed in the vicinity of the tube center (Fig. 1). The coil was

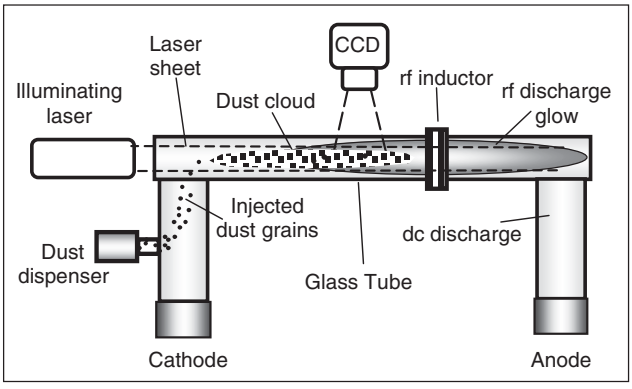


FIG. 1. Scheme of the PK-4 plasma chamber and of the experiment on cluster formation.

 

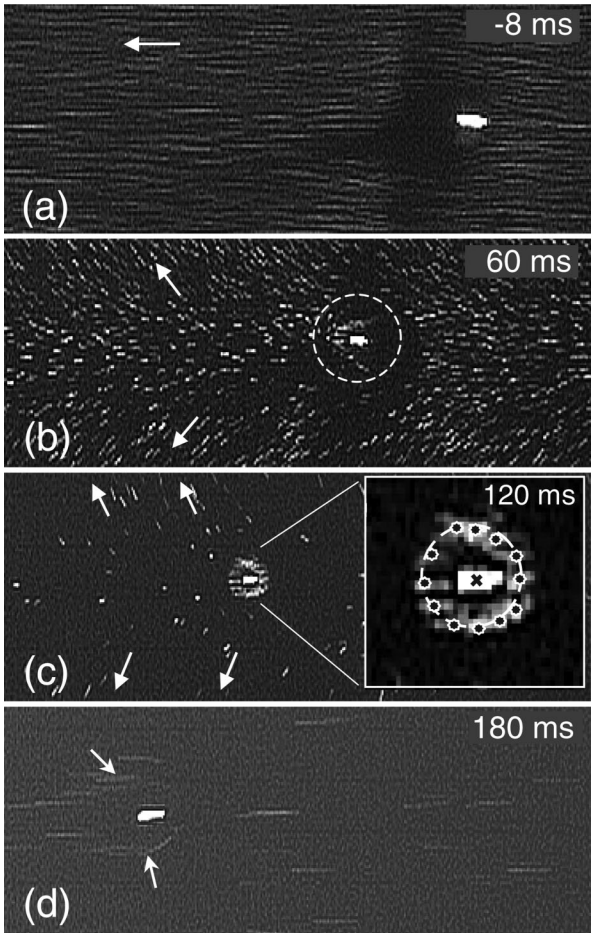


FIG. 2. Cluster formation and destruction in the central part of the discharge tube. (a) Dust cloud in the uniform positive dc column just before the rf pulse: the arrow shows the direction of particle drift, the bright point is the big particle. (b) 60 ms after the rf-pulse ignition: beginning of the cluster formation, arrows show dispersing of small particles, dashed circle shows a sphere of attraction of small particles. (c) 120 ms after the rf-pulse ignition: formation of cluster is complete, arrows show drift of residual small particles, the insert shows an enlarged image of the cluster with 12 identified small particles. (d) Just after the ending of rf pulse: the cluster is disrupted instantaneously, arrows show small particles dispersed from former cluster. The area shown is about $7 \times 3$ mm$^2$.

powered by an rf current at a frequency of 81.36 MHz and a power of 1.5 W. Under microgravity monodisperse melamine formaldehyde dust particles with a radius of $r_{p2} = 1.28$ $\mu$m were injected into the dc discharge plasma in the vicinity of the cathode. Being injected, the charged dust particles drifted to the anode due to the dc electric field of the discharge of about 2 V/cm. The injected particles were illuminated by a laser sheet of 150 $\mu$m width and recorded by a CCD camera with an image resolution of $640 \times 240$ pix (binning mode) and a frame rate of 120 frames per second (8.3 ms per frame). The camera field of view (FoV) was $12.6 \times 9.5$ mm$^2$ at the tube axis. During the experiments the injected small particles formed an elongated drifting uniform dust cloud with a diameter of 1.5 cm and a particle density of $n_d \sim 2 \times 10^{11}$ m$^{-3}$, which was confined along the tube axis by the radial electric field in the cylindrical dc positive column. In addition to the injected small particles, heavy dust particle conglomerates randomly appeared in the dc discharge and FoV. These conglomerates were formed on the tube surface in the vicinity of the dispenser and they could easily be distinguished from the original 1.28 $\mu$m particles by their different behavior and high brightness on the recorded images [Fig. 2(a)]. As soon as the heavy particles appeared in the FoV, an experimentalist manually initiated an rf discharge pulse of a rectangular shape with a duration of $\tau_0 = 180$ ms. This duration was chosen to achieve a stationary state of the cluster after the pulse ignition (response times of small and big particles were 3 and 16 ms, respectively) as well as to investigate a cluster disordering process after the pulse completion. The unperturbed electron density $n_{e0} \approx n_{i0}$ and electron temperature $T_e$ for both discharge modes were diagnosed by a Langmuir probe in laboratory investigations [10] and presented in Table I. The ion temperature $T_i$ under current conditions is about the neutral gas temperature $T_n$. Just after the rf discharge ignition [Fig. 2(b)], the plasma density $n_{i0}$, $n_{e0}$ rapidly increased by a factor of 20, the small particle drift velocity was reduced from 5 cm/s to 1 cm/s, and all small dust particles started to drift away from the tube axis to the tube walls due to the increased radial ion drag forces. Only the heavy conglomerates randomly approaching the tube axis kept their positions due to their sufficiently high inertia. At the same time, the small particles randomly situated within a sphere of 500 $\mu$m around the big particle were attracted to it and fixed at distances of about 200 $\mu$m. After 120 ms [Fig. 2(c)], the formation of the cluster was completed due to the absence of other small particles in its vicinity, and the cluster had acquired a stable spherical shape with the big particle in the center. A cluster structure is presented in the insert of Fig. 2(c), showing a cross section of the cluster

TABLE I. Measured electron number density $n_e$ and electron temperature $T_e$; ion Debye length $r_{Di}$; calculated ion currents $I_{p1}$ and $I_{p2}$ and particle charge numbers $Z_{p1}$ and $Z_{p2}$ [11] for the particles with radii of $r_{p1} = 6$ $\mu$m and $r_{p2} = 0.64$ $\mu$m, respectively, for the dc and combined dc-rf discharge modes.

| Discharge modes | $n_e$, m$^{-3}$ | $T_e$, eV | $r_D$, $\mu$m | $I_{p1}$, s$^{-1}$ | $I_{p2}$, s$^{-1}$ | $Z_{p1}$ | $Z_{p2}$ |
|---|---|---|---|---|---|---|---|
| dc | $(2 \pm 0.5) \times 10^{14}$ | $7 \pm 1$ | 85 | $2.1 \times 10^{10}$ | $2.7 \times 10^{8}$ | 19000 | 1600 |
| dc-rf | $(4 \pm 1) \times 10^{15}$ | $3.5 \pm 0.5$ | 19 | $1.3 \times 10^{11}$ | $1.9 \times 10^{9}$ | 22000 | 1850 |

by the laser. Analyzing Fig. 2(c) one should remember that the cluster is moving and its image is slightly spread in a horizontal direction due to the finite exposure time. About 12 small particles can be recognized in this cross section corresponding to a total amount in the cluster shell of about 30 with a cluster radius of $R_{cl} = 190 \pm 20$ $\mu$m. Note, that the cluster is almost spherical, indicating isotropic conditions in the bulk plasma. During the next 60 ms (7 video frames) of the rf pulse the cluster slightly moved along the tube axis due to the presence of a small neutral gas flow, keeping, however, its spherical structure. Finally, as soon as the rf pulse was finished after 180 ms and the discharge had returned to its pure dc mode, the cluster was rapidly disrupted during 1 frame (8 ms) via an electrostatic explosion due to the rapid reduction of the plasma density [Fig. 2(d)], while the other small dust particles started to return to the tube center. The effective radius of the big particle $r_{p1} = 6 \pm 2.5$ $\mu$m was determined from the measured response time $\tau_{p1} = 16 \pm 5$ ms of the big particle on the rf-pulse disturbance.

A scheme of the formed cluster is presented in Fig. 3, which is similar to Fig. 2 of Ref. [6]. A formation of the cluster after increasing the plasma density and its rapid disruption (even explosion) with decreasing plasma density reveals the important role of the plasma fluxes for the particle linking in the cluster. The experiment showed that already the first small particles coming to the big particle were stopped at a distance of about $r = R_{cl}$. Therefore, for simplicity we restrict our consideration to the pair interaction of the big particle with one small particle; i.e., we consider a small test particle in the field of the big particle. For the equilibrium position of a small particle at $r = R_{cl}$ from the big particle one can write

$$|F_{pd}(R_{cl})| = |F_e(R_{cl})|, \tag{1}$$

where $F_{pd} = F_{id} + F_{ed}$ is the attractive plasma drag force, $F_{id}$ and $F_{ed}$ are the ion and the electron drag forces,

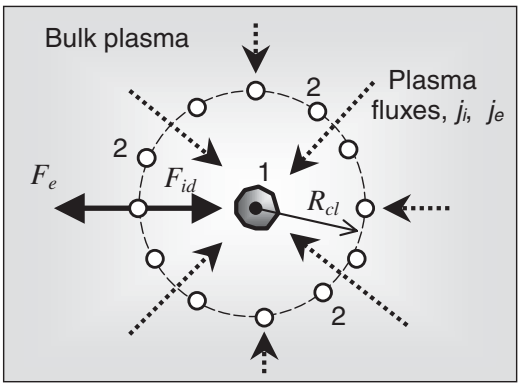


FIG. 3. Scheme of cluster: 1-central big particle, 2-small bound particles; dotted arrows are plasma fluxes. $F_{id}$-attracting ion drag force; $F_e$-electrostatic repulsion from the central particle.

respectively, acting on the small particle by the plasma flowing onto the big particle, and $F_e$ is the repulsive electrostatic force. Because of the small electron mass, $F_{id} \gg F_{ed}$ [12], so $F_{pd} \cong F_{id}$. Knowing the dependences $F_{id}(r)$ and $F_e(r)$, one can explain the observed equilibrium position of the small particle at $r = R_{cl}$. The ion drag force $F_{id}(r)$ is determined by the ion flux $j_{i1}(r) = n_i(r)u_i(r) = I_{p1}/4\pi r^2$ flowing onto the big particle, where $I_{p1}$ is the total ion current onto the big particle. The ion currents $I_{p1}$ and $I_{p2}$ as well as the particle charge numbers $Z_{p1}$ and $Z_{p2}$ for both dc and dc-rf discharge modes were calculated by the particle in cell (PIC) method [11] taking into account rare ion-neutral collisions (in our case the ion mean free path $\lambda_{in} \approx 80$ $\mu$m and $\lambda_{Di} \approx 19$ $\mu$m $\ll \lambda_{in}$ in the dc-rf discharge mode). The results are presented in Table I. Then we find $u_i(R_{cl}) \approx 70$ m/s, i.e., the ion flow at $r = R_{cl}$ is subthermal. Based on the ion drag force measurements performed earlier [13] in our discharge chamber for the pressure range of 20–120 Pa and the recent fully self-consistent numerical ion drag force calculations in the entire range of charge-exchange collisionality [14] one can conclude, that the ion drag force $F_{id}$ can be calculated in the binary collision approximation in the moderate ion-grain coupling regime [12] with the particle charge number $Z_{p2}$ calculated by the PIC method [11]

$$|F_{id}| = (2\sqrt{2}/3)m_i n_i u_i v_{T_i} r_{p2}^2 z_{p2}^2 \tau^2 \Lambda_{id}, \tag{2}$$

where $m_i$ is the ion mass, $v_{Ti} = (T_i/m_i)^{-1/2}$, $r_{p2}$, $z_{p2} = |Z_{p2}|e^2/4\pi\varepsilon_0 r_{p2} T_e$, and $Z_{p2}$ are the radius, normalized charge and "PIC" charge number of the small particle, respectively, $\Lambda_{id} = 2z_{p2}\int_0^\infty e^{-zx}\ln[1 + 2\tau^{-1}(\lambda_{Di}/r_{p2})x]dx$, and $\varepsilon_0$ is the vacuum permittivity. According to [11], the ratio $n_i(r)/n_{i0}$ is about unity at $r \geq 5r_D \approx 100$ $\mu$m, i.e., in the region of interest with $r \approx 200$ $\mu$m. Having all the data for Eq. (2), we have calculated $F_{id} = 3.3 \times 10^{-14}$ N for $r = R_{cl}$. Note, that as soon as the ion flux $j_{i1}(r) \sim r^{-2}$ and $u_i(R_{cl}) = 70$ m/s $\ll v_{Ti} = 350$ m/s, the dependence $F_{id}(r)$ is also described by the power law function $F_{id}(r) \sim r^{-2}$ [12]. Such a dependence will hold in the region of $r \geq r_{min} \approx 100$ $\mu$m, where $u_i(r) < v_{Ti}$. Estimations have shown that the plasma ionization essentially affects the above calculated ion flux $j_{i1}(r)$ only at $r > 500$ $\mu$m. To complete Eq. (1), we need to evaluate the repulsive electrostatic force $F_e(r) = Z_{p2}ed\phi_e(r)/dr|_{r=Rcl}$, where $\phi_e(r)$ is the electrostatic potential distribution around the big grain. This potential was calculated self-consistently by a direct solution of the kinetic equation for ion motion with the Bhatnagar-Gross-Krook collision term using the Green's function in the spherically symmetrical case [15]. The calculated profile $\phi_e(r)$ is presented in Fig. 4. It has a clear physical meaning: (i) $\phi_e(r)$ has a Debye-Hückel form with $\phi_e(r_{p1}) = \phi_{s1}$ in agreement with Ref. [11] and with an effective screening length $r_{scr} \approx 1.6r_{Di}$ at $r_{p1} \leq r < 2r_{Di}$; (ii) $\phi_e(r)$ asymptotically approaches the

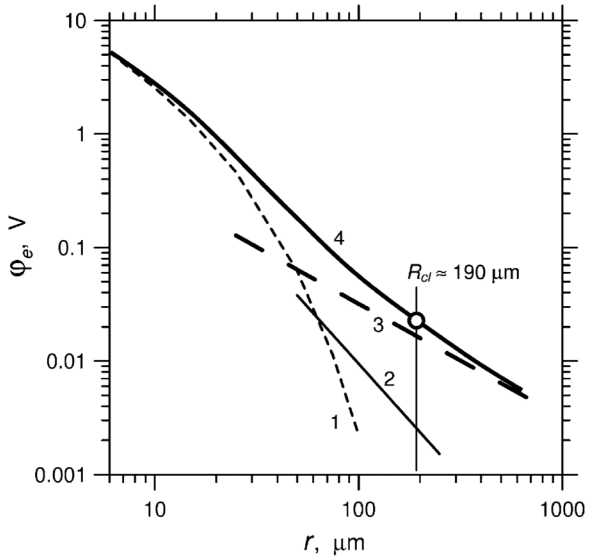


FIG. 4. Electrostatic potential around the big particle calculated in different approximations: (1) Debye-Hückel potentials with the linearized ion Debye length $r_{Di} = 19$ $\mu$m; (2) unscreened potential $\varphi_e^{**}(r) = eZ_{p1}r_{p1}/8\pi\varepsilon_0 r^2$ due to the OML ion current on the big particle in the collisionless regime; (3) $\varphi_e^{*}(r) = 3.2 \times 10^{-6}(\mathrm{V} \times \mathrm{m})/r$ which supports ion current to the big particle in the mobility regime; (4) self-consistent numerical calculation.

profile $\varphi_e^{*}(r) = 3.2 \times 10^{-6}(\mathrm{V} \cdot \mathrm{m})/r$ at large distances $r > 15r_{Di}$, which supports the ion drift $u_i = \mu_i(d\varphi_e^{*}/dr)$ (neon ion mobility is $\mu_i = 0.78$ m$^2$/V $\times$ s for a pressure of 60 Pa [16]) to the big particle with a total ion current of $I_{p1} = 1.3 \times 10^{11}$ s$^{-1}$; (iii) $\phi_e(r)$ changes from the Debye-Hückel form to the power law form $\varphi_e^{*}(r)$ at intermediate distances $2r_{Di} < r < 10r_{Di}$. According to the obtained profiles $F_i(r)$ and $F_e(r)$ the small particle will move as described in the following scenario. At large distances ($r \gg R_{cl}$) one obtains $F_{id}/F_e \approx 1.3$, corresponding to an attraction of the small particle to the big particle. As the small particle approaches from infinity to $r = R_{cl}$, the force $F_e \sim d\phi_e(r)/dr$ starts to grow faster than $r^{-2}$, but the force $F_{id}(r)$ still keeps its dependence $r^{-2}$. As $r$ decreases from infinity to $R_{cl} \approx 10r_{Di}$, the ratio $F_{id}/F_e$ diminishes from 1.3 to 1, and the small particle finally finds its equilibrium position at $r = R_{cl}$. Note, that even in our weekly collisional plasma ($\lambda_{in} \approx 4r_D$) rare ion-neutral collisions sufficiently increase the profile $\phi_e(r)$ [and the ion flux $j_{i1}(r)$] with respect to those calculated in the orbit motion limited (OML) approximation [17] for $r \gg r_{Di}$ as $\varphi_e^{**}(r) = eZ_{p1}r_{p1}/8\pi\varepsilon_0 r^2$ (Fig. 4). After the end of the rf pulse, the ion current $I_{p1}$ is reduced by a factor of 6 (Table I), the attractive force $F_{id}$ becomes much less then the repulsive force $F_e$, and the cluster quickly disperses into the plasma. Note, that the ratio $F_{id}/F_e$ is not very sensitive to the radius $r_{p1}$, because both $F_{id}$ and $F_e$ are proportional to the electric field induced by the big particle.

In conclusion, in the present work an attraction of negatively charged micron-sized particles in a low-pressure gas-discharge plasma was observed under microgravity conditions. This experiment is characterized by the following features: (i) the interacting microparticles are *microbodies* in the plasma, i.e., particle sizes $r_p \ll r_D \ll \lambda_{in}$; (ii) the particles are *floating* objects in the plasma; (iii) the particle attraction was observed in the *bulk* region of the plasma, where isotropic plasma conditions exist, confirmed by the spherical form of the cluster; (iv) the observable particle attraction with an increasing plasma density and the rapid cluster disruption with a decreasing plasma density reveal the important role of the *plasma flux forces* for the particle linking in the boundary-free cluster; (v) ionization processes in the plasma lead to a principal restriction of the particle attraction range.

This work was supported by DLR under grant 50 WM 0504, by European Space Agency at the 41st parabolic flight campaign, and by the Russian Foundation for Basic Research Grants No. 06-02-17520-a and No. 07-02-01464-a. The authors appreciate the excellent engineering support throughout this work by Karl Tarantik and Christian Deysenroth from the Max-Planck-Institut für extraterrestrische Physik.

*Corresponding author.
†usachev@ihed.ras.ru

[1] H. M. Thomas and G. E. Morfill, Nature (London) **379**, 806 (1996).
[2] V. E. Fortov *et al.*, Phys. Usp. **47**, 447 (2004).
[3] V. N. Tsytovich, Phys. Usp. **50**, 409 (2007).
[4] V. N. Tsytovich *et al.*, Comments Plasma Phys. Controlled Fusion **17**, 249 (1996).
[5] A. M. Ignatov, Plasma Phys. Rep. **22**, 585 (1996).
[6] J. Goree *et al.*, Phys. Rev. E **59**, 7055 (1999).
[7] D. Samsonov *et al.*, Phys. Rev. E **63**, 025401(R) (2001).
[8] M. Klindworth *et al.*, Phys. Rev. Lett. **93**, 195002 (2004).
[9] S. V. Vladimirov and M. Nambu, Phys. Rev. E **52**, R2172 (1995).
[10] V. Fortov *et al.*, Comments Plasma Phys. Controlled Fusion **47**, B537 (2005).
[11] A. V. Zobnin *et al.*, JETP **91**, 483 (2000).
[12] S. A. Khrapak *et al.*, Phys. Rev. E **70**, 056405 (2004).
[13] V. Yaroshenko *et al.*, Phys. Plasmas **12**, 093503 (2005).
[14] L. Patacchini and I. H. Hutchinson, Phys. Rev. Lett. **101**, 025001 (2008).
[15] A. V. Zobnin *et al.*, Phys. Plasmas **15**, 043705 (2008).
[16] L. S. Frost, Phys. Rev. **105**, 354 (1957).
[17] J. E. Allen, Phys. Scr. **45**, 497 (1992).